Regular article

Performance of density functionals for calculation of reductive ring-opening reaction energies of Li$^+$-EC and Li$^+$-VC

Young-Kyu Han, Sang Uck Lee

Computational Chemistry Laboratory, Corporate R&D, LG Chem Ltd, Research Park, 305–380, Daejon, Korea

Abstract. Reaction energies were determined for reductive ring-opening reactions of Li$^+$-coordinated ethylene carbonate (EC) and vinylene carbonate (VC) by using various density functional theory (DFT) and ab-initio methods applying the basis sets up to Dunning's aug-cc-pVQZ. The methods examined include the local density functional (SVWN), the pure gradient-corrected density functionals (BLYP and BPW91), and the hybrid density functionals (B3LYP, B1LYP, B3PW91, and mPW1PW91). Comparison of the DFT results with ab-initio results indicates that the mPW1PW91 approach introduced by Adamo and Barone, is superior to all the other DFT methods (including B3LYP). The performance of more cost-effective Pople-type basis sets ranging from 6-31G(d,p) to 6-311 + +G(3df,3pd) was assessed at DFT levels of theory by calibrating them with the aug-cc-pVQZ results

Keywords: Density functional theory – Performance – Ring-opening reaction – Cyclic carbonate – Lithium-ion battery

Introduction

A hybrid lithium-ion battery system is made up of a graphite anode, a non-aqueous organic electrolyte that acts as an ionic path between the electrodes, and a transition metal oxide cathode. Lithium-ion battery electrolytes typically consist of a lithium salt and various additives dissolved in an organic solvent. The most popular solvents are the mixtures of cyclic carbonates, for example, ethylene carbonate (EC), propylene carbonate (PC), and linear carbonates such as dimethyl carbonate (DMC). It is generally recognized that organic electrolytes, particularly cyclic carbonates, are decomposed, during the first several lithium intercalations, into graphite, to form a solid electrolyte interface (SEI) film between the graphite anode surface and the electrolyte. The SEI film plays a crucial role that affects the capacity, cycle life, and safety of the lithium-ion rechargeable battery [1, 2]. Thus, the mechanism of solvent decomposition and subsequent SEI build-up have been widely studied in the lithium-ion battery electrolyte, both experimentally [3, 4, 5, 6, 7, 8, 9, 10, 11] and theoretically [12, 13, 14, 15, 16, 17, 18, 19, 20]. It has been demonstrated that electrons are initially transferred from the polarized electrode to the Li$^+$-coordinated solvent (or additive) molecules, forming ion-pair intermediates. Ring-opening of the intermediates then occurs, generating radical anions which participate in termination reactions resulting in Li organic or inorganic salts, building up the SEI film [16, 17, 18, 19, 20].

The elucidation of reaction mechanisms is a major challenge for theoretical studies. To date, many theoreticians have used quantum chemical methods to gain insights into the initial reactions at the microscopic level [12, 13, 14, 16, 17, 18, 19, 20]. Density functional theory (DFT)-based approaches were mainly employed along with Pople-type basis sets ranging from 6-31G(d) to 6-311 + +G(d,p) in such calculations, but it is not clear which functional should be used, and what the accuracy of the functional with a given basis set would be. Obtaining more accurate results than DFT results calls for a more elaborate ab-initio treatment such as coupled-cluster singles, doubles, and perturbative triples (CCSD(T)) [21]. However, this requires too much computational resource for such systems with C$_1$ molecular symmetry. The main objective of the present study is to investigate the performance of different DFT methods when dealing with reductive ring-opening reactions. Because of the lack of experimental information for comparison, we will use the results obtained in high-level ab-initio Møller–Plesset second-order perturbation (MP2) [22] and CCSD(T) calculations as a suitable

Correspondence to: Young-Kyu Han
e-mail: ykhan@lgchem.com

reference. In order to minimize the error caused by the basis set incompleteness, the diffuse-function augmented correlation-consistent basis sets [23] were employed up to aug-cc-pVQZ. Results were also obtained with the more cost-effective Pople-type basis sets ranging from 6-31G(d,p) to 6-311++G(3df,3pd), and they were calibrated against the aug-cc-pVQZ results. The results of this work may be useful for other workers in choosing the basis sets for DFT calculations.

In the present work, various DFT, ab-initio MP2, and CCSD(T) calculations were used to investigate the reductive ring-opening reactions of Li^+-coordinated EC and vinylene carbonate (VC). The molecular structures of EC and VC are depicted in Fig. 1. The EC molecule is the electrolyte solvent most widely used in lithium-ion rechargeable batteries. The VC molecule is a reactive additive that reacts on the anode. Spectroscopic studies indicate that VC polymerizes on the lithiated graphite surfaces, thus forming poly alkyl Li-carbonate species that suppress both solvent and salt anion reduction [24]. We have studied reductive ring-opening reactions by C_1–O_2 and O_2–C_3 bond cleavage for Li^+-EC and Li^+-VC. Recently, Wang et al. investigated reductive decomposition by O_2–C_3 bond cleavage for Li^+-EC [16] and Li^+-VC [19] at the B3PW91/6-311++G(d,p) level of theory, and our results are compared with theirs. Details of the calculations are given in the next section, and the results and discussion are then presented.

Calculation details

Hartree–Fock (HF)/6–311+G(d) calculations were performed for geometry optimization of local minima and transition states. The transition states were confirmed by the sole imaginary frequency and primary intrinsic reaction coordinate (IRC) [25] calculations. Single-point energies were calculated at the various DFT, ab-initio MP2, and CCSD(T) levels of theory using the HF optimized geometries. Occupied and virtual orbitals except for the $1s$ orbitals of carbons and oxygens are fully correlated at the ab-initio correlated levels of theory. Kohn–Sham DFT calculations were performed with seven different exchange correlation functionals, namely, the local density approximation (LDA:SVWN [26, 27]), the generalized gradient approximation (GGA:BLYP [28, 29] and BPW91 [30]), and the hybrid functionals (B3LYP [31], B1LYP [32], B3PW91, and mPW91PW91 [33]). Carbon, oxygen,

hydrogen, and lithium were treated with the Dunning correlation-consistent polarized valence basis sets, cc-pVDZ, cc-pVTZ, and cc-pVQZ, where D, T, and Q refer to the number of contracted functions in each valence subshell, and Dunning correlation-consistent polarized valence basis sets with diffuse functions, aug-cc-pVDZ, aug-cc-pVTZ, and aug-cc-pVQZ [23]. For the most accurate CCSD(T) calculations, cc-pVDZ, aug-cc-pVDZ, and cc-pVTZ basis sets were used for practical reasons. Because lithium does not carry a negative charge in any of the complexes we considered here, its basis set was not augmented with diffuse functions. Six Pople-type basis sets [34] (6-31G(d,p), 6-311G(d,p), 6-311++G(d,p), 6-311++G(2d,2p), 6-311++G(3d,3p), and 6-311++G(3df,3pd)) including diffuse (denoted by "+") and polarization functions (denoted by "d", "p", "f") were also employed at the B3PW91 and mPW1PW91 levels of theory. A spin-unrestricted scheme was employed for the odd numbered electron systems. The stationary point wave functions were also checked for spin contamination by evaluation of the $<S^2>$ values. The Gaussian98 [35] program package was employed to perform the DFT and ab-initio calculations.

Results and discussion

For the reductive ring-opening reactions of Li^+-EC, the mechanisms considered are shown in Fig. 2 together with selected structural data. In sharp contrast to an isolated EC molecule, Li^+-EC is much more easily reduced, bringing about an ion-pair intermediate **2** [16]. An electron was transferred to EC in **2**, and the CO_3 group does not keep the planar structure due to the change of the carbonyl C hybridization from sp^2 in **1** to nearly sp^3 in **2**. Ring-opening reactions by C_1–O_2 (**2** → **4** → **5**) and O_2–C_3 cleavage (**2** → **3** → **6**) could occur, leading to radical anions coordinated with lithium cation **5** and **6** (or **7**), respectively. Table 1 lists the reaction energies for Li^+-EC computed at the various DFT, and ab-initio MP2, and CCSD(T) levels of theory. The $1s$ orbitals of carbon and oxygen atoms were frozen in our ab-initio calculations. At the CCSD(T)/aug-cc-pVDZ level, the errors due to the frozen-core approximation were calculated to be small, i.e. average errors are less than 0.1 kcal mol^{-1} for the energy quantities reported here. To assess the accuracy of the CCSD(T) data, T_1 diagnostic [36] values were computed for the CCSD wavefunctions. A value of T_1 below 0.02 is indicative of a CCSD(T) result closely approximating the full configuration interaction limit. The T_1 diagnostic values are less than 0.02 except for 0.027 for the transition-state structure **3**, demonstrating that our CCSD(T) results are quite reliable.

The effectiveness of the basis set extension is quite different in wavefunction-based theories and density-based theories. The convergence with respect to the basis set size is much faster with the density-based methods than with the post-HF methods. This has already been
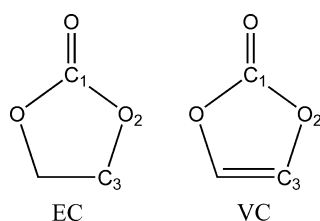

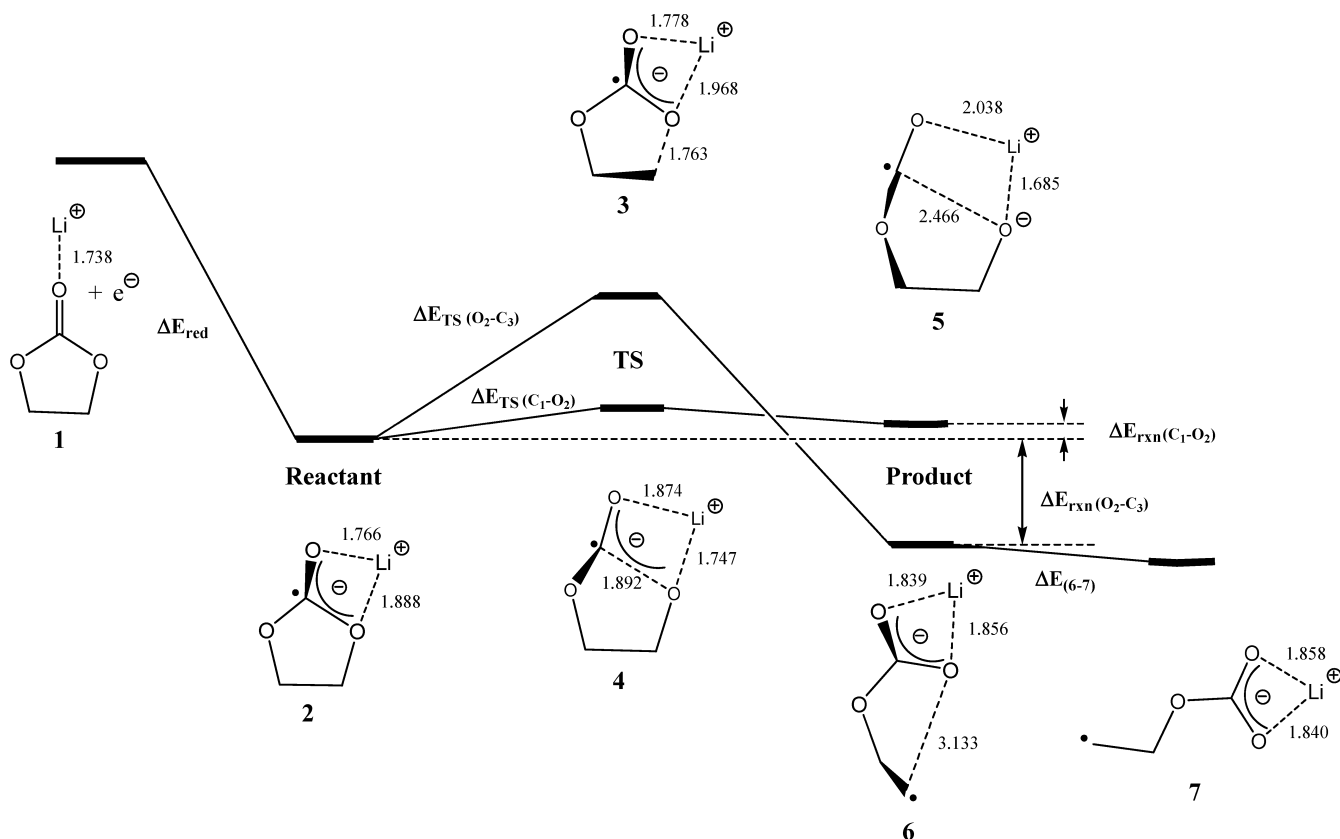**Fig. 1.** Labelling and molecular structures of EC and VC

Fig. 2. Mechanisms for the reductive ring-opening reactions of Li$^+$-EC: *1*, singlet state, *2–7*, doublet states

found in other comparative studies [37, 38, 39, 40]. It follows from the fact that in the DFT approach the orbitals are only needed to construct the density. The mean deviations of the cc-pVDZ results with respect to the aug-cc-pVQZ results are 1.16 (maximum deviation 3.05) kcal mol^{-1} and 2.59 (8.77) kcal mol^{-1} for the B3LYP and MP2 levels of theory, respectively. However, the mean (maximum) deviations of aug-cc-pVTZ results are largely reduced to 0.10 (0.15) kcal mol^{-1} and 0.19 (0.43) kcal mol^{-1} for the B3LYP and MP2 levels, respectively. This implies that one can perform meaningful comparisons between the results from DFT and post-HF methods, provided that the basis set having at least aug-cc-pVTZ quality is employed.

The most reliable CCSD(T) calculations are expensive and could be performed only for cc-pVDZ, aug-cc-pVDZ, and cc-pVTZ basis sets. The CCSD(T)/aug-cc-pVQZ results were estimated from the CCSD(T)/cc-pVTZ results and the MP2 energy variations upon the basis set extension from cc-pVTZ to aug-cc-pVQZ on the basis of the fact that the energy variations at the MP2 level are very similar to those at the CCSD(T) level. It should be mentioned that the energy variations at the MP2 level are quite different from those at the CCSD(T) level for $\Delta E_{rxn}(O_2–C_3)$. Thus, we calculated the $\Delta E_{rxn}(O_2–C_3)$ value at the CCSD(T) level of theory using aug-cc-pVTZ to assess the performance of DFT calculations through comparisons of the aug-cc-pVTZ results for $\Delta E_{rxn}(O_2–C_3)$.

Judging from the absolute mean deviations and maximum deviations with respect to the estimated CCSD(T)/aug-cc-pVQZ values, the quality of DFT results for the reaction energies is in the order SVWN < BLYP < BPW91 < B3LYP < B1LYP < B3PW91 < mPW1PW91. The hybrid functionals provide much better agreement with the estimated CCSD(T) results than the LDA and pure GGA functionals. Among the hybrid functionals, the mPW1PW91 method gives by far the best results with only a 0.57 (0.98) kcal mol^{-1} mean (maximum) difference, followed by the B3PW91 method with a 0.61 (2.31) kcal mol^{-1} deviation. The LDA method shows very poor performance, and the performance of pure GGA is found to be unsatisfactory. Both the BLYP and BPW91 methods significantly underestimate the activation barrier energies. The most popular B3LYP also somewhat underestimates the ΔE_{TS} values and gives quite a large mean deviation of 2.09 (3.38) kcal mol^{-1}. The MP2 $\Delta E_{TS}(O_2–C_3)$ value is rather high compared with the estimated CCSD(T) value. These may explain the large discrepancy (6.5 kcal mol^{-1}) between the B3LYP and MP2 $\Delta E_{TS}(O_2–C_3)$ values for Li-EC reported in Ref. [20]. The $\Delta E_{TS}(C_1–O_2)$ values are positive or negative depending upon the calculation methods. We have optimized the structure **2** at the BLYP, B3LYP, mPW1PW91, and MP2 levels of theory using cc-pVTZ. The BLYP calculation gives a long

Table 1. Comparison of reaction energies(kcal mol⁻¹) for reductive ring-opening of Li⁺-EC with various DFT and ab initio levels of theory

	SVWN	BLYP	BPW91	B3LYP	B1LYP	mPW1 PW91	B3PW91	HF	MP2	CCSD(T)[a]
ΔE_{red}										
cc-pVDZ	−100.11	−89.28	−88.56	−89.53	−86.20	−87.57	−87.54	−69.00	−78.55	−80.93
aug-cc-pVDZ	−103.88	−92.66	−91.70	−92.94	−89.59	−90.69	−90.67	−71.54	−86.44	−88.91
cc-pVTZ	−101.92	−90.18	−89.63	−90.50	−87.09	−88.44	−88.53	−68.79	−84.47	−86.61
aug-cc-pVTZ	−102.85	−91.20	−90.53	−91.41	−88.00	−89.28	−89.35	−69.30	−86.94	
cc-pVQZ	−102.38	−90.69	−90.04	−90.95	−87.54	−88.80	−88.90	−68.98	−86.25	
aug-cc-pVQZ	−102.71	−91.04	−90.36	−91.27	−87.86	−89.10	−89.19	−69.18	−87.32	(−89.46)
$\Delta E_{TS}(O_2\text{-}C_3)$										
cc-pVDZ	10.91	9.18	9.90	13.70	14.78	15.72	14.36	31.35	19.58	16.68
aug-cc-pVDZ	9.51	7.52	8.45	12.10	13.15	14.26	12.96	29.46	17.24	14.67
cc-pVTZ	9.70	7.75	8.76	12.55	13.65	14.83	13.46	30.71	19.11	16.09
aug-cc-pVTZ	9.41	7.40	8.46	12.21	13.30	14.50	13.16	30.26	18.17	
cc-pVQZ	9.62	7.65	8.67	12.46	13.56	14.73	13.38	30.52	18.76	
aug-cc-pVQZ	9.51	7.50	8.55	12.32	13.42	14.60	13.26	30.36	18.60	(15.57)
$\Delta E_{TS}(C_1\text{-}O_2)$										
cc-pVDZ	2.72	−2.15	−0.57	−0.36	−0.20	1.73	1.08	3.70	0.36	0.58
aug-cc-pVDZ	3.32	−1.77	−0.03	0.30	0.48	2.54	1.84	4.61	0.57	0.82
cc-pVTZ	2.58	−2.55	−0.63	−0.31	−0.10	2.11	1.37	4.64	1.73	1.98
aug-cc-pVTZ	2.77	−2.34	−0.42	−0.09	0.13	2.32	1.59	4.73	1.74	
cc-pVQZ	2.63	−2.49	−0.60	−0.25	−0.04	2.13	1.40	4.56	1.70	
aug-cc-pVQZ	2.74	−2.37	−0.48	−0.13	0.09	2.26	1.52	4.64	1.69	(1.95)
$\Delta E_{rxn}(O_2\text{-}C_3)$										
cc-pVDZ	−11.73	−21.69	−21.29	−24.37	−25.26	−23.57	−23.72	−37.82	−27.33	−26.18
aug-cc-pVDZ	−13.28	−23.80	−22.60	−25.78	−26.62	−24.38	−24.55	−37.68	−26.69	−25.91
cc-pVTZ	−14.98	−25.81	−24.19	−27.48	−28.27	−25.63	−25.93	−38.39	−26.61	−26.15
aug-cc-pVTZ	−14.79	−25.77	−23.98	−27.29	−28.08	−25.37	−25.64	−38.09	−26.14	−25.73
cc-pVQZ	−14.98	−25.94	−24.25	−27.52	−28.31	−25.67	−25.93	−38.41	−26.49	
aug-cc-pVQZ	−14.88	−25.87	−24.15	−27.42	−28.22	−25.57	−25.82	−38.31	−26.01	
$\Delta E_{rxn}(C_1\text{-}O_2)$										
cc-pVDZ	9.31	−0.96	2.43	1.35	1.23	5.17	4.28	1.79	1.77	1.75
aug-cc-pVDZ	10.56	−0.16	3.49	2.46	2.36	6.52	5.57	3.24	3.18	3.19
cc-pVTZ	9.02	−1.84	2.13	1.02	0.96	5.36	4.37	2.73	4.52	4.48
aug-cc-pVTZ	9.31	−1.53	2.43	1.34	1.28	5.66	4.66	2.86	4.76	
cc-pVQZ	9.10	−1.79	2.16	1.06	1.00	5.38	4.39	2.55	4.51	
aug-cc-pVQZ	9.23	−1.66	2.29	1.21	1.14	5.52	4.52	2.66	4.63	(4.59)
$\Delta E(6\text{–}7)$										
cc-pVDZ	−0.14	0.18	0.12	−0.02	−0.04	−0.03	−0.05	−0.22	0.24	0.33
aug-cc-pVDZ	−0.49	−0.13	−0.18	−0.29	−0.31	−0.30	−0.32	−0.40	0.22	0.29
cc-pVTZ	−0.47	−0.11	−0.22	−0.29	−0.31	−0.35	−0.36	−0.47	0.12	0.17
aug-cc-pVTZ	−0.65	−0.30	−0.36	−0.45	−0.47	−0.48	−0.49	−0.56	−0.02	
cc-pVQZ	−0.58	−0.23	−0.30	−0.39	−0.41	−0.43	−0.45	−0.55	−0.01	
aug-cc-pVQZ	−0.64	−0.28	−0.34	−0.43	−0.45	−0.46	−0.47	−0.56	−0.04	(0.02)
Avg. dev.	6.06	3.43	2.46	2.09	1.98	0.57	0.61	8.77	0.99	0.00
Max. dev.	13.24	8.07	7.03	3.38	3.45	0.98	2.31	20.29	3.02	0.00

[a]The values in parentheses are estimated CCSD(T)/aug-cc-pV-QZ values

bond length of 2.27 Å for the C_1–O_2 bond, whereas the lengths were 1.64 Å, 1.55 Å, and 1.57 Å for B3LYP, mPW1PW91, and MP2, respectively, indicating that there is no activation barrier at the BLYP/cc-pVTZ level of theory.

The $<S^2>$ values are 0.76 for the reaction energies at the HF level, except for 0.85 for the transition-state structure **3**. For the DFT calculations, the $<S^2>$ values are very close to 0.75 with the maximum value of 0.76 at the mPW1PW91 level for the structure **3**. We believe that major conclusions would be affected very little by the spin-contamination errors.

Let us now turn to the reaction energies for the reductive ring-opening of Li⁺-VC. Table 2 lists the reaction energies computed at the DFT, MP2, and CCSD(T) levels of theory. The T_1 diagnostic values (0.015~0.035) for Li⁺-VC and Li-VC are somewhat larger than those for Li⁺-EC and Li-EC (0.014~0.027),

where the largest value is 0.035 for the transition-state structure **3**. Nevertheless, it is noteworthy that the performance of the functionals is very similar to the Li⁺-EC case. Among the functionals, mPW1PW91 is the best with a small deviation of 0.34 (1.16) kcal mol⁻¹, followed by B3PW91 with a deviation of 0.57 (1.62) kcal mol⁻¹. The B3LYP method gives a larger deviation of 1.95 (4.08) kcal mol⁻¹ and somewhat underestimates the ΔE_{TS} values. It should be noted that the MP2 deviation, 3.18 (9.45) kcal mol⁻¹, is very large. Such a large deviation seems to be closely related with the large spin-contamination of the HF wavefunctions for structures **3**, **6**, and **7**. Namely, the $<S^2>$ values are 0.99, 0.95, and 0.96 for structure **3**, **6**, and **7**, respectively, at the HF level, which may be responsible for the large deviation of MP2 for the $\Delta E_{TS}(O_2$–$C_3)$ and $\Delta E_{rxn}(O_2$–$C_3)$ values. The $<S^2>$ values are close to 0.75 for the other structures at the HF level of theory. It is widely-known that MP2 is

Table 2. Comparison of reaction energies (kcal mol^{-1}) for reductive ring-opening of Li$^+$-VC with various DFT and ab initio levels of theory

	SVWN	BLYP	BPW91	B3LYP	B1LYP	mPW1PW91	B3PW91	HF	MP2	CCSD(T)[a]
ΔE_{red}										
cc-pVDZ	−102.61	−93.19	−92.32	−93.09	−89.76	−90.85	−91.01	−73.49	−80.90	−84.00
aug-cc-pVDZ	−106.92	−97.45	−96.12	−97.46	−94.17	−94.84	−94.91	−77.33	−89.50	−92.38
cc-pVTZ	−104.88	−94.80	−93.86	−94.83	−91.47	−92.31	−92.57	−74.18	−87.34	−90.16
aug-cc-pVTZ	−106.02	−96.15	−95.00	−96.09	−92.74	−93.45	−93.64	−75.09	−90.22	
cc-pVQZ	−105.38	−95.42	−94.33	−95.42	−92.08	−92.79	−93.02	−74.60	−89.40	
aug-cc-pVQZ	−105.85	−96.00	−94.83	−95.94	−92.59	−93.28	−93.47	−74.96	−90.52	(−93.34)
$\Delta E_{TS}(O_2\text{-}C_3)$										
cc-pVDZ	20.38	17.89	18.68	22.35	23.34	24.49	23.14	37.61	32.77	23.84
aug-cc-pVDZ	19.43	16.77	17.80	21.50	22.50	23.78	22.44	36.73	31.47	22.45
cc-pVTZ	19.66	16.96	18.05	21.90	22.95	24.30	22.90	37.91	33.92	24.47
aug-cc-pVTZ	19.59	16.88	18.02	21.89	22.95	24.29	22.90	37.93	33.46	
cc-pVQZ	19.67	16.97	18.07	21.97	23.04	24.35	22.97	38.03	34.10	
aug-cc-pVQZ	19.69	16.99	18.10	22.01	23.08	24.39	23.00	38.05	34.07	(24.62)
$\Delta E_{TS}(C_1\text{-}O_2)$										
cc-pVDZ	0.67	−2.44	−1.47	−1.25	−1.11	0.13	−0.32	1.82	−0.74	−0.61
aug-cc-pVDZ	0.89	−2.41	−1.28	−0.94	−0.78	0.58	0.08	2.42	−0.67	−0.55
cc-pVTZ	0.48	−2.82	−1.60	−1.26	−1.09	0.37	−0.15	2.50	0.11	0.23
aug-cc-pVTZ	0.57	−2.72	−1.47	−1.12	−0.95	0.51	−0.02	2.57	0.13	
cc-pVQZ	0.48	−2.83	−1.61	−1.24	−1.07	0.37	−0.15	2.46	0.14	
aug-cc-pVQZ	0.55	−2.74	−1.52	−1.15	−0.97	0.46	−0.06	2.52	0.12	(0.24)
$\Delta E_{rxn}(O_2\text{-}C_3)$										
cc-pVDZ	3.09	−7.07	−6.34	−9.51	−10.46	−8.53	−8.63	−27.18	−6.85	−12.06
aug-cc-pVDZ	1.62	−9.11	−7.58	−10.70	−11.59	−9.12	−9.29	−26.39	−6.33	−12.03
cc-pVTZ	0.58	−10.40	−8.56	−11.75	−12.59	−9.81	−10.08	−26.63	−4.58	−10.69
aug-cc-pVTZ	0.77	−10.32	−8.29	−11.50	−12.34	−9.47	−9.73	−26.15	−4.35	−10.63
cc-pVQZ	0.55	−10.52	−8.60	−11.76	−12.59	−9.80	−10.04	−26.50	−4.07	
aug-cc-pVQZ	0.71	−10.37	−8.41	−11.58	−12.41	−9.61	−9.85	−26.29	−3.80	
$\Delta E_{rxn}(C_1\text{-}O_2)$										
cc-pVDZ	5.85	−6.48	−2.95	−5.87	−6.45	−2.15	−2.77	−11.35	−6.11	−6.14
aug-cc-pVDZ	7.11	−5.92	−1.90	−4.72	−5.25	−0.56	−1.29	−9.17	−3.40	−3.58
cc-pVTZ	5.87	−7.28	−2.96	−5.89	−6.39	−1.48	−2.24	−9.63	−2.06	−2.33
aug-cc-pVTZ	6.39	−6.76	−2.46	−5.33	−5.82	−0.93	−1.71	−9.16	−1.22	
cc-pVQZ	6.00	−7.24	−2.94	−5.81	−6.30	−1.41	−2.18	−9.62	−1.69	
aug-cc-pVQZ	6.20	−7.03	−2.72	−5.59	−6.08	−1.19	−1.97	−9.43	−1.25	(−1.51)
$\Delta E(6\text{–}7)$										
cc-pVDZ	−0.46	−0.85	−1.16	−1.46	−1.58	−1.71	−1.65	−2.89	−1.61	−1.69
aug-cc-pVDZ	−1.18	−1.63	−1.83	−2.12	−2.23	−2.30	−2.24	−3.40	−2.04	−2.14
cc-pVTZ	−1.02	−1.48	−1.74	−2.01	−2.12	−2.24	−2.17	−3.37	−2.09	−2.23
aug-cc-pVTZ	−1.18	−1.66	−1.90	−2.15	−2.26	−2.37	−2.30	−3.45	−2.12	
cc-pVQZ	−1.14	−1.60	−1.83	−2.10	−2.21	−2.32	−2.25	−3.42	−2.14	
aug-cc-pVQZ	−1.18	−1.64	−1.87	−2.13	−2.24	−2.35	−2.28	−3.44	−2.15	(−2.30)
avg. dev.	6.33	3.29	2.29	1.95	1.64	0.34	0.57	9.78	3.18	0.00
max. dev.	12.51	7.63	6.52	4.08	4.57	1.16	1.62	18.38	9.45	0.00

[a] The values in parentheses are estimated CCSD(T)/aug-cc-pV-QZ values

more susceptible to spin-contamination than DFT or CCSD(T) methods [41]. For the DFT calculations, the $<S^2>$ values are close to 0.75 with the maximum value of 0.77 at the mPW1PW91 level for the structure **7**.

It is practically difficult to use the aug-cc-pVTZ basis set or a larger one for investigating solvent (or additive) decomposition for large systems (> 30 atoms) even at DFT levels of theory. Instead, Pople-type 6-31G(d,p) and 6-311 + +G(d,p) basis sets have often been employed for large and small-sized molecular systems, respectively. To assess the quality of Pople-type basis sets at the DFT level, we have calculated the reaction energies of the reductive ring-opening reactions of Li$^+$-EC and Li$^+$-VC using several Pople-type basis sets ranging from 6-31G(d,p) to 6-311 + +G(3df,3pd) at the B3PW91 and mPW1PW91 levels of theory, and compared the results with the aug-cc-pVQZ results in

Table 3. We also obtained the reaction energies at the mPW1PW91/6-311 + +G(3df,3pd)//mPW1PW91/6–311 +G(d) level of theory (Table 3). The results are in good agreement with the mPW1PW91/6-311 + +G(3df,3pd)// HF/6–311 + G(d) results with a difference of 0.51 (1.96) kcal mol^{-1}. Recently, Wang et al. reported the reaction energies for the O$_2$–C$_3$ ring-opening reactions of Li$^+$-EC [16] and Li$^+$-VC [19] at the B3PW91/6-311 + +G(d,p) level of theory. Our B3PW91/6-311 + +G(d,p)//HF/6–311 + G(d) results are in good agreement with their results with a small difference of 0.2 (0.4) kcal mol^{-1}. These imply that the reaction energies are not strongly sensitive to the optimization method for obtaining geometries.

Table 4 summarizes the average and maximum absolute deviations from the aug-cc-pVQZ results for all the basis sets used in the present work. The deviations

111

Table 3. Reaction energies (kcal mol^{-1}) computed at the B3PW91 and mPW1PW91 levels of theory using the Pople-type basis sets

Li$^+$-EC	ΔE_{red}	ΔE_{TS} (O$_2$–C$_3$)	ΔE_{TS} (C$_1$–O$_2$)	ΔE_{rxn} (O$_2$–C$_3$)	ΔE_{rxn} (C$_1$–O$_2$)	ΔE(6–7)	Deviation[a]
B3PW91							
6–31G(d,p)	−87.87	14.13	1.94	−23.79	6.06	0.03	1.11 (2.03)
6–311G(d,p)	−88.59	13.45	0.69	−26.14	3.62	0.09	0.57 (0.83)
6–311++G(d,p)	−90.57	13.02	0.94	−26.11	3.60	−0.26	0.60 (1.38)
6–311++G(2d,2p)	−90.21	12.65	1.36	−26.40	4.27	−0.41	0.45 (1.02)
6–311++G(3d,3p)	−89.82	12.89	1.41	−26.01	4.48	−0.42	0.23 (0.63)
6–311++G(3df,3pd)	−89.11	13.23	1.58	−25.88	4.52	−0.45	0.04 (0.08)
aug-cc-pVQZ	−89.19	13.26	1.52	−25.82	4.52	−0.47	0.00 (0.00)
mPW1PW91							
6–31G(d,p)	−87.92	15.44	2.61	−23.62	7.00	0.06	1.05 (1.95)
6–311G(d,p)	−88.55	14.86	1.41	−25.80	4.59	0.10	0.56 (0.93)
6–311++G(d,p)	−90.56	14.39	1.67	−25.81	4.57	−0.25	0.61 (1.46)
6–311++G(2d,2p)	−90.19	13.98	2.09	−26.15	5.24	−0.40	0.47 (1.09)
6–311++G(3d,3p)	−89.80	14.23	2.15	−25.74	5.47	−0.41	0.24 (0.70)
6–311++G(3df,3pd)	−89.09	14.58	2.32	−25.60	5.52	−0.43	0.02 (0.06)
aug-cc-pVQZ	−89.10	14.60	2.26	−25.57	5.52	−0.46	0.00 (0.00)
6–311++G(3df,3pd)[b]	−88.93	14.35	1.88	−26.10	4.44	−0.50	
B3PW91							
6–31G(d,p)	−91.34	23.19	0.31	−8.32	−1.08	−1.95	0.91 (2.13)
6–311G(d,p)	−92.40	22.53	−0.52	−10.54	−3.43	−1.86	0.76 (1.46)
6–311++G(d,p)	−94.78	22.47	−0.38	−10.45	−3.01	−2.13	0.66 (1.31)
6–311++G(2d,2p)	−94.66	22.29	−0.11	−10.63	−2.34	−2.33	0.53 (1.19)
6–311++G(3d,3p)	−94.34	22.45	−0.13	−10.41	−2.21	−2.28	0.38 (0.87)
6–311++G(3df,3pd)	−93.52	22.97	−0.01	−10.02	−2.00	−2.25	0.06 (0.17)
aug-cc-pVQZ	−93.47	23.00	−0.06	−9.85	−1.97	−2.28	0.00 (0.00)
mPW1PW91							
6–31G(d,p)	−91.25	24.54	0.78	−8.16	−0.41	−2.00	0.85 (2.03)
6–311G(d,p)	−92.16	23.95	−0.01	−10.27	−2.69	−1.92	0.77 (1.50)
6–311++G(d,p)	−94.64	23.88	0.15	−10.19	−2.27	−2.18	0.67 (1.36)
6–311++G(2d,2p)	−94.52	23.66	0.41	−10.39	−1.60	−2.39	0.54 (1.24)
6–311++G(3d,3p)	−94.21	23.83	0.39	−10.15	−1.44	−2.34	0.39 (0.93)
6–311++G(3df,3pd)	−93.38	24.36	0.52	−9.75	−1.23	−2.31	0.07 (0.14)
aug-cc-pVQZ	−93.28	24.39	0.46	−9.61	−1.19	−2.35	0.00 (0.00)
6–311++G(3df,3pd)[b]	−93.14	23.67	0.47	−10.42	−3.19	−2.33	

[a] Mean (maximum) deviation
[b] mPW1PW91/6–311++G(3df,3pd)//mPW1PW91/6–311+G(d) results

for Pople-type DZP (double-zeta polarization) basis set, 6-31G(d,p), are close to those for cc-pVDZ basis set. On the other hand, the quality of Pople-type TZP + (*sp* diffuse-augmented triple-zeta polarization) basis set turned out to be similar to that of aug-cc-pVDZ basis set, rather than aug-cc-pVTZ basis set. The combination of DFT with the Pople-type basis set having at least a 6-311++G(3d,3p) quality gives accurate DFT results within a 1 kcal mol^{-1} deviation. It is noteworthy that the results using the 6-311++G(3df,3pd) basis set are very close to the aug-cc-pVQZ results, whose performance is better than larger-size of aug-cc-pVTZ and cc-pVQZ basis sets. We strongly suggest that the 6-311++G(3df,3pd) basis set be used to cost-effectively explore the basis-set limit in DFT calculations for systems similar to those considered in this work. We tested the performance of the BH&HLYP functional using 6-311++G(3df,3pd), since some studies have reported that accurate predictions of activation energies have been shown for the functional [42, 43]. However, the performance of the functional turned out to be poor with deviations of 2.35 (4.17) and 2.59 (4.89) kcal mol^{-1}, respectively, for calculating the reductive ring-opening reaction energies of Li$^+$-EC and Li$^+$-VC. The BH&HLYP ΔE_{TS}(O$_2$–C$_3$) values are rather higher, by about 4∼5 kcal mol^{-1}, compared with the estimated CCSD(T) values.

Conclusions

The performance of seven commonly used density functionals (SVWN, BLYP, BPW91, B3LYP, B1LYP, mPW1PW91, and B3PW91) was studied with Pople- and Dunning-type basis sets. Based on overall mean DFT versus CCSD(T) deviations, the mPW1PW91 functional furnishes the best performance among the DFT methods for predicting the reaction energies for reductive ring-opening of Li$^+$-coordinated EC and VC. DFT has an advantage over MP2, when errors caused by slow basis set convergence and spin-contamination are considered. However, the performance of LDA and pure GGA functionals is unsatisfactory, and the most popular B3LYP is not recommendable. The performance of widely-used 6-31G(d,p) and 6-311++G(d,p) basis sets is comparable to that of cc-pVDZ and aug-cc-pVDZ, respectively, and they are still practical basis sets particularly for large systems. The 6-311++G(3d,3p) and cc-pVTZ basis sets were at least required to achieve high accuracy, within a deviation of 1 kcal mol^{-1} in

Table 4. Average and maximum deviations for the results using the various basis sets with respect to the aug-cc-pVQZ results at the mPW1PW91 level of theory

	Avg. dev.	Max. dev.	N_{basis}[a]
Li^+-EC			
6–31G(d,p)	1.05	1.95	118
6–311G(d,p)	0.56	0.93	150
6–311 + +G(d,p)	0.61	1.46	182
6–311 + +G(2d,2p)	0.47	1.09	229
6–311 + +G(3d,3p)	0.24	0.70	276
6–311 + +G(3df,3pd)	0.02	0.06	345
cc-pVDZ	0.99	2.00	118
aug-cc-pVDZ	0.76	1.58	188
cc-pVTZ	0.23	0.66	266
aug-cc-pVTZ	0.12	0.20	398
cc-pVQZ	0.14	0.30	505
aug-cc-pVQZ	0.00	0.00	719
Li^+-VC			
6–31G(d,p)	0.85	2.03	108
6–311G(d,p)	0.77	1.50	138
6–311 + +G(d,p)	0.67	1.36	168
6-311 + +G(2d,2p)	0.54	1.24	209
6–311 + +G(3d,3p)	0.39	0.93	250
6–311 + +G(3df,3pd)	0.07	0.14	309
cc-pVDZ	0.92	2.43	108
aug-cc-pVDZ	0.58	1.56	170
cc-pVTZ	0.29	0.97	238
aug-cc-pVTZ	0.12	0.26	352
cc-pVQZ	0.18	0.49	445
aug-cc-pVQZ	0.00	0.00	627

[a]Number of basis set

DFT calculations. The basis-set limit could be obtained practically by using the 6-311 + +G(3df,3pd) basis set.

References

1. Dominey LA (1994) Lithium batteries. new materials, developments and perspectives. Elsevier, Amsterdam
2. Mogi RD, Inaba M, Iriyama Y, Abe T, Ogumi Z (2003) J Power Sources 119–121:597
3. Peled E, Golodnitsky D, Menachem C, Bar-Tow D (1998) J Electrochem Soc 145:3482
4. Aurbach D, Levi MD, Levi E, Schechter A (1997) J Phys Chem B 101:2195
5. Aurbach D, Ein-Eli Y, Zaban A (1994) J Electrochem Soc 141:L1
6. Aurbach D, Ein-Eli Y, Chusid O, Carmeli Y, Babai M, Yamin H (1994) J Electrochem Soc 141:603
7. Shu ZX, McMillan RS, Murray JJ (1993) J Electrochem Soc 140:922
8. Arora P, White RE, Doyle M (1998) J Electrochem Soc 145:3647
9. Aurbach D, Moshkovich M, Cohen Y, Schechter A (1999) Langmuir 15:2947
10. Schechter A, Aurbach D, Cohen H (1999) Langmuir 15:3334
11. Aurbach D (2000) J Power Sources 89:206
12. Endo E, Ata M, Tanaka K, Sekai K (1998) J Electrochem Soc 145:3757
13. Endo E, Tanaka K, Sekai K (2000) J Electrochem Soc 147:4029
14. Li T, Balbuena PB (2000) Chem Phys Lett 317:421
15. Marquez A, Balbuena PB (2001) J Electrochem Soc 148:A624
16. Wang Y, Nakamura S, Ue M, Balbuena PB (2001) J Am Chem Soc 123:11708
17. Wang Y, Balbuena PB (2002) J Phys Chem B 106:4486
18. Wang Y, Balbuena PB (2002) J Phys Chem A 106:9582
19. Wang Y, Nakamura S, Tasaki K, Balbuena PB (2002) J Am Chem Soc 124:4408
20. Han YK, Lee SU, Ok JH, Cho JJ, Kim HJ. (2002) Chem Phys Lett 360:359
21. Pople JA, Head-Gordon M, Raghavachari K (1987) J Chem Phys 87:5968
22. Møller C, Plesset MS (1934) Phys Rev 46:618
23. Dunning Jr TH (1989) J Chem Phys 90:1007
24. Aurbach D, Gamolsky K, Markovsky B, Gofer Y, Schmidt M, Heider U (2002) Electrochim Acta 47:1423
25. Gonzalez C, Schlegel HB (1989) J Chem Phys 90:2154
26. Slater JC (1974) Quantum theory of molecular and solids, vol 4: the self-consistent field for molecular and solids. McGraw–Hill, New York
27. Vosko SH, Wilk L, Nusair M (1980) Can J Phys 58:1200
28. Becke AD (1998) Phys Rev A 38:3098
29. Lee C, Yang W, Parr RG (1988) Phys Rev B 37:785
30. Perdew JP, Wang Y (1992) Phys Rev B 45:13244
31. Becke AD (1993) J Chem Phys 98:5648
32. Becke AD (1996) J Chem Phys 104:1040
33. Adamo C, Barone V (1998) J Chem Phys 108:664
34. Hehre WJ, Ditchfield R, Pople JA (1972) J Chem Phys 56:2257
35. Frisch MJ, Trucks GW, Schlegel HB, Scuseria GE, Robb MA, Cheeseman JR, Zakrzewski VG, Montgomery Jr JA, Stratmann RE, Burant JC, Dapprich S, Millam JM, Daniels AD, Kudin KN, Strain MC, Farkas O, Tomasi J, Barone V, Cossi M, Cammi R, Mennucci B, Pomelli C, Adamo C, Clifford S, Ochterski J, Petersson GA, Ayala PY, Cui Q, Morokuma K, Malick DK, Rabuck AD, Raghavachari K, Foresman JB, Cioslowski J, Ortiz JV, Baboul AG, Stefanov BB, Liu G, Liashenko A, Piskorz P, Komaromi I, Gomperts R, Martin RL, Fox DJ, Keith T, Al-Laham MA, Peng CY, Nanayakkara A, Challacombe M, Gill PMW, Johnson B, Chen W, Wong MW, Andres JL, Gonzalez C, Head-Gordon M, Replogle ES, Pople JA (1998) Gaussian 98, Rev. A.7. Gaussian Inc, Pittsburgh, PA
36. Lee TJ, Taylor PR (1989) Int J Quantum Chem Symp 23:199
37. Gill PMW, Johnson BG, Pople JA, Frisch MJ (1992) Chem Phys Lett 197:499
38. Hertwig H, Koch W (1995) J Comput Chem 16:576
39. Scheiner C, Baker J, Andzelm JW (1997) J Comput Chem 18:775
40. Martin ML, El-Yazal J, Francois JP (1995) Mol Phys 86:1437
41. Baker J, Scheiner A, Andzelm J (1993) Chem Phys Lett 216:380
42. Zhang Q, Bell R, Truong TN (1995) J Phys Chem 99:592
43. Durant JL (1996) Chem Phys Lett 256:595